

# Fatigue Behaviour of Friction Stir Welded Rolled Thick Plates of AA7075-T651 Aluminium Alloy Joints

<sup>1</sup>P. Sivaraj, Assistant Professor, <sup>2</sup> D. Kanagarajan, Assistant Professor, <sup>3</sup>V. Balasubramanian, Professor, Department of Manufacturing Engineering, Annamalai University, Annamalai Nagar – 608 002, Tamil Nadu, India

## ABSTRACT

The fatigue strength of welded joints represents the core problem for their industrial applications. Friction stir welding (FSW) demonstrated the enhancement of fatigue resistance for aluminium alloys, with respect to traditional fusion techniques. The aim of the present work is to evaluate the fatigue properties of 12 mm thick AA 7075 -T651 aluminium alloy plates joined by friction stir welding (FSW) process. The fatigue properties were evaluated under uniaxial tensile loading condition (stress ratio = 0.1, Frequency=10Hz) at room temperature using servo-hydraulic controlled machine. The fatigue endurance (S-N) curves of the welded joints and unwelded parent metal were constructed. The resultant fatigue properties were correlated with the tensile, hardness and microstructural characteristics of welded joints. The mode of failure was analyzed through scanning electron microscopy. It is found that the fatigue life of friction stir welded AA 7075- T651 Aluminium alloy joints is appreciably lower than unwelded parent metal but it is higher than fusion welded joints.

**Keywords:** AA 7075 aluminium alloy; friction stir welding; fatigue, microstructure.

## 1.0 INTRODUCTION

High-strength, precipitation-hardenable 7000-series aluminium alloys such as alloy AA 7075 are used extensively in military and aircraft primary structures. This alloy derives its strength from precipitation of Mg<sub>2</sub>Zn and Al<sub>2</sub>CuMg phases. The assembly of metals has been a fundamental topic for many years. Major problem with this alloy is that, it is not fusion weldable. In particular, this class of aluminium alloy is difficult to join by conventional fusion welding practices because the dendritic structure formed in the fusion zone can seriously deteriorate the mechanical properties of the joint. It is extremely sensitive to weld solidification cracking as well as heat-affected zone (HAZ) liquation cracking due to the presence of copper. Though, it is possible to overcome the problem of weld solidification cracking using a suitable non heat- treatable aluminium alloy filler (for example, Al-Mg or Al-Si), the resulting joint efficiencies are unacceptably low [1].

At the beginning of the 1990s, Friction Stir Welding (FSW), a new joining process developed by The Welding Institute (TWI), UK [2], has emerged as a promising solid state process with the potential to join aluminium alloys which are traditionally considered unweldable. Because material subjected to FSW does not melt and recast, the resultant weldment offers advantages over conventional arc weldments such as better retention of baseline mechanical properties, less distortion, lower residual stresses, and fewer weld defects. Friction stir welding achieves solid phase joining by locally introducing frictional heat and plastic flow by rotation of the welding tool with resulting local microstructure changes in aluminium alloys [3-7]. For the aircraft components fatigue performance was known to be one of the crucial assessment qualities, therefore many efforts have been done to investigate the fatigue properties of friction stir welded various aluminium alloy joints [8-10].

The effects of three welding processes on the tensile, fatigue and corrosion behaviour of AA 2219 were studied by Malarvizhi et al., [11]. The results showed that the FSW joints exhibited superior tensile and fatigue properties compared to EBW and GTAW joints. Mechanical and microstructural properties of dissimilar 2024 and 7075 aluminium alloy sheets of 2.5 mm thick friction stir welded joints were investigated by Cavaliere et al., [12]. It was reported that for the most common alloys, the fatigue strength decreases as the welding speed / rotating speed ratio is higher. Balasubramanian et al., [1] studied the effects of pulsed current and post weld ageing treatment on fatigue crack growth behaviour of AA 7075 aluminium alloy of 6 mm thick rolled plates using GTAW and GMAW processes and reported that the pulsing of current and simple post weld ageing treatment increased the fatigue crack growth resistance and fatigue life.

Tianwen and Yanyao [13] conducted fatigue testing on AA 7075–T651 aluminium alloy under uniaxial, torsion and axial-torsion loading conditions and given a fatigue model which can predict the fatigue life for most experiments. The fatigue life of friction stir welded 10 mm thick plates of aluminium alloy 5083 was investigated by Caizhi Zhou et al., [14]. It was reported that the fatigue life was found to be 9–12 times longer than that of MIG-pulse welds under  $R = 0.1$  and the fatigue characteristic values of each welds have been increased from 39.8 MPa for MIG to 67.3 MPa for FSW. Tensile and fatigue properties of 4 mm thick 2198 Al–Li alloy friction stir welded sheets were investigated by Cavaliere et al., [15]. Srivatsan et al., [16] evaluated the fracture behavior of aluminium alloy 7055 base material. Temmar et al., [17] reports the influence of post-weld aging treatment on the microstructure, tensile strength, hardness and Charpy impact energy of GTAW joints of 2.5 mm thickness 7075 T6 aluminium alloy. The tensile properties, microhardness, microstructure and fracture surface morphology of the GMAW, GTAW and FSW joints of RDE 40 aluminium alloy was evaluated and the results were compared by Lakshminarayanan and Balasubramnaian [18]. However, the fatigue data available for FSW joints of higher thickness (>10 mm) AA 7075-T651 was deficient despite the numerous applications involved using this alloy. Since, the fatigue failures are normally starts from the surface, the crack propagation depends on the thickness (size effect) of the

component. So, understanding the fatigue behavior of higher thickness plates of AA 7075-T651 is necessary at this current scenario. Hence, the present investigation is aimed to study the fatigue behaviour of 12 mm thick plates of AA 7075-T651 aluminium alloy butt joints made by FSW process. The resultant fatigue properties are compared with its base metal fatigue properties.

## 2.0 MATERIALS AND EXPERIMENTAL PROCEDURE

Rolled plates of 12 mm thick aluminium alloy (AA 7075 in T651 condition) were used in this investigation. The chemical composition of base metal is presented in **Table 1**. **Fig.1** shows the experimental details. **Fig. 1a** and **Fig.1b** represents the FSW tool diagram and tool photographs respectively. Prior to welding, the abutting faces of the plates were finely milled in order to avoid surface scaling intruded with the tool. The FSW tool with tapered threaded pin profile of shoulder diameter of 36 mm, pin diameter of 12 mm and pin length of 11.6 mm was used in this study. Few trial experiments were made to identify the parameters which give the defect free welds and those parameters were taken as the optimized welding parameters in this investigation. Tool rotation and welding speeds were taken as 350 rpm 25 mm/min, respectively. Necessary care was taken to avoid joint distortion during welding. The welding was carried out normal to the rolling direction of the base metal. **Fig. 1c** and **Fig. 1d** shows the fabricated joint photographs and schematic specimen extraction plan respectively.

The welded joints were sliced using power hacksaw to prepare fatigue and tensile test specimens. Two different fatigue specimens were prepared to evaluate the fatigue properties as per ASTM E467-08 specifications. Unnotched specimens were prepared to evaluate fatigue limit and notched specimens were prepared to evaluate the fatigue notch factor and notch sensitivity factor. The fatigue testing experiments were conducted at six different stress levels (100, 150, 200, 250, 300 and 350 MPa) and all the experiments were conducted under uniaxial tensile loading condition (stress ratio = 0.1, Frequency=10Hz) using servo hydraulic fatigue testing machine (Make: INSTRON, UK; Model: 8801). Two different tensile specimens were prepared as per the ASTM E8M-04 standard guidelines. The unnotched and notched tensile

**Table 1 : Chemical composition (wt.%) of Aluminium Alloy AA7075-T651**

Zn	Mg	Cu	Fe	Si	Mn	Cr	Ti	Al
6.1	2.9	2.0	0.50	0.4	0.30	0.28	0.20	Bal



## Discover the Power of Powder®

As a key component in the manufacturing of coated welding electrodes and cored welding wires, iron powder can have a direct influence on both welding properties and quality of the final weld metal.

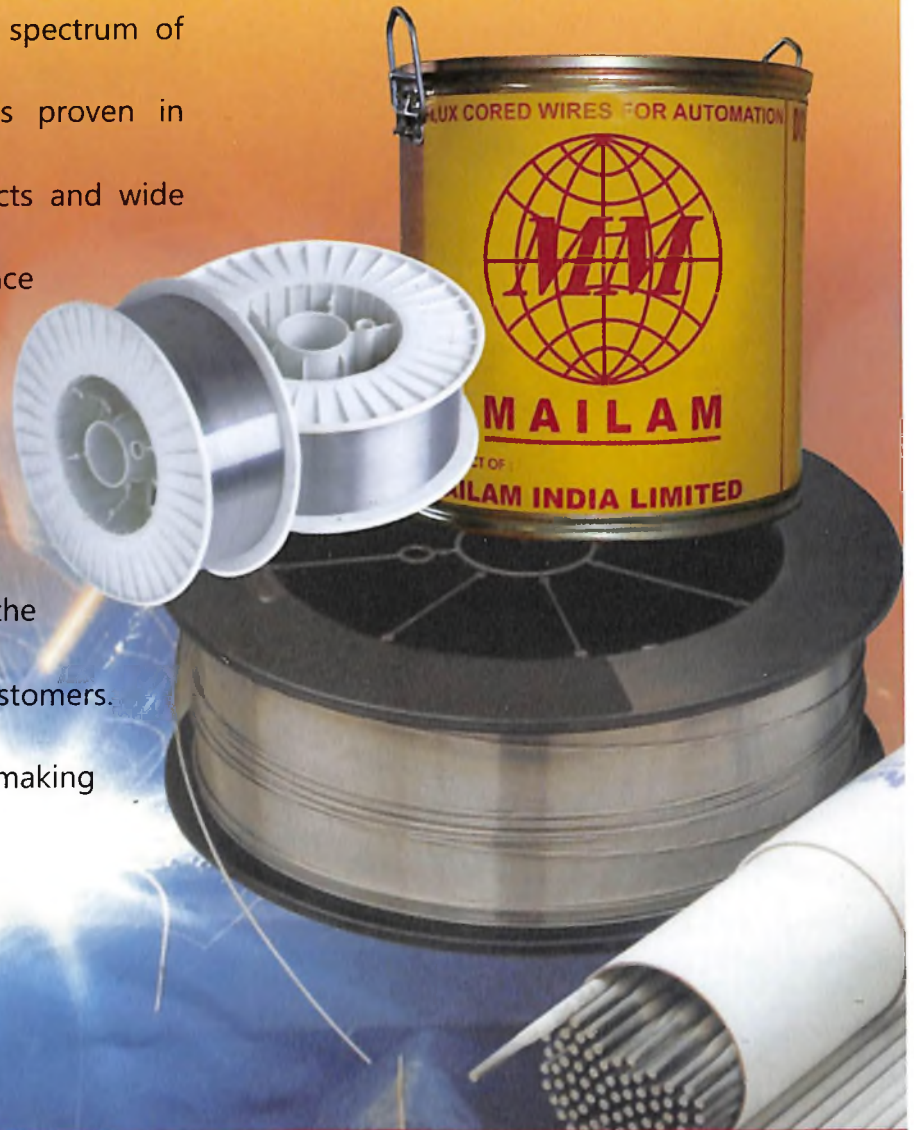
Explore the most comprehensive range of iron powders for welding applications. We provide consistent high-quality products and reliable services that ensure optimum manufacturing of coated electrodes and cored wires.

# High performance welding consumables for your application

Mailam offers entire spectrum of welding consumables proven in critical nuclear projects and wide range of maintenance applications.

Our emphasis is on quality and reliability which makes Mailam the preferred choice of customers.

We are committed to making a better weld.



**Welding Consumables Destination**



**MAILAM INDIA LIMITED**

Mailam Main Road, Sedarapet, Pondicherry - 605 111.

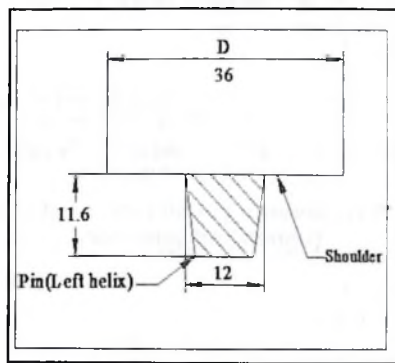
Tel : 91 413 2677311, 2677074, Fax: 91 413 2677089

E-Mail: [mailam@mailamindia.com](mailto:mailam@mailamindia.com), URL : [www.mailamindia.com](http://www.mailamindia.com)

**ISO 9001 Certified, by BSI**

specimens were prepared as per Fig. 1e and Fig. 1f respectively to evaluate yield strength, tensile strength, percentage elongation and notch tensile strength. Tensile testing was carried out using 100 kN, electro mechanical controlled universal testing machine (Make: FIE-Blue star, India; Model: UNITEK-94100). The 0.2% offset yield strength was derived from the load displacement curve. Hardness measurement was done across the weld center line by Vickers micro hardness tester (SHIMADZU, Japan Model: HMV-2T) with 0.05 kg load and 15 s dwell time.

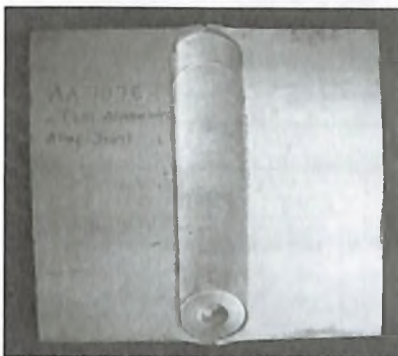
The specimen for metallographic examination was sectioned to the required sizes from the joint regions and polished using different grades of emery papers. Final polishing was done using the diamond compound (1 $\mu$ m particle size) in the disc polishing machine. Metallographic specimens were prepared by standard metallographic technique and were etched with Keller's reagent (150 ml H<sub>2</sub>O, 3 ml HNO<sub>3</sub> and 6 ml HF). The etching solution was cooled to 0°C and specimens were etched for about 20 s in order to study the grain structure of the weld zones and to allow for optical microscopy characterizations



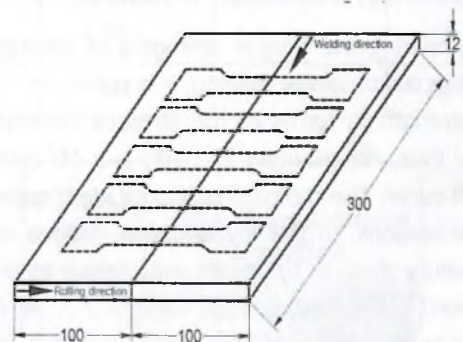
(a) FSW Tool Diagram



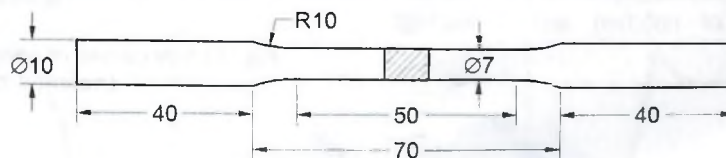
(b) FSW Tool Photograph



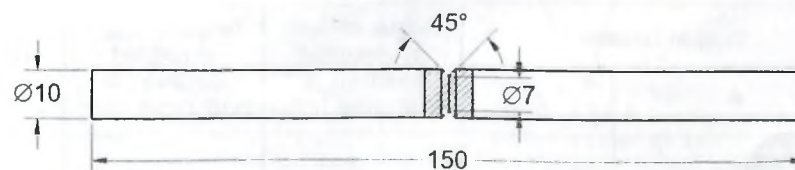
(c) Fabricated Joint



(d) Scheme of welding and specimen extraction diagram



(e) Dimension of unnotched fatigue/tensile specimens



(f) Dimension of notched fatigue/tensile specimens

(all dimensions are in "mm")

**Fig. 1 : Experimental details**

reveal the macro and microstructure. The micro structural analysis was done using optical microscope (MEIJI, Japan; Model: MI7100). The HRSEM analysis was carried out to identify the fracture mode of tested specimen. The electron dispersive X-ray (EDAX) analysis was also undertaken using QUANTA 3D FEG system to determine the composition of specific elements in the material being joined.

**3.0 RESULTS**

**3.1 Fatigue properties**

**Fig. 2** shows the S-N curves of unnotched fatigue specimens of unwelded parent metal and friction stir welded AA7075 aluminium alloy joints. The S-N curve in the high cycle fatigue region is generally described by the Basquin equation [19].

$$S^n N = A \quad (1)$$

Where 'S' is the stress amplitude, 'N' is the number of cycles to failure, and, 'n' and 'A' are empirical constants. Each S-N curve shown in **Fig.2** and **Fig.3** can be represented by the above equation. From those equations, the empirical constants 'n' (slope of the curve) and 'A' (intercept of the curve) were evaluated and they are presented in **Table 2**.

When comparing the fatigue strengths of different welded joints subjected to similar loading, it is convenient to express fatigue strength in terms of the stresses corresponding to particular lives, for example 10<sup>5</sup>, 10<sup>6</sup>, and 10<sup>7</sup> cycles on the mean S-N curve. The choice of reference life is quite arbitrary. For these reasons, in this investigation, fatigue strength of welded joints at 2 X 10<sup>6</sup> cycles was taken as a basis for comparison. The stress corresponding to 2 X 10<sup>6</sup> cycles was taken as an indication of the endurance limit and it was evaluated for all the joints and is presented in **Table 2**. The effect of notches on fatigue strength was determined by comparing the S-N curves of notched and unnotched specimens.

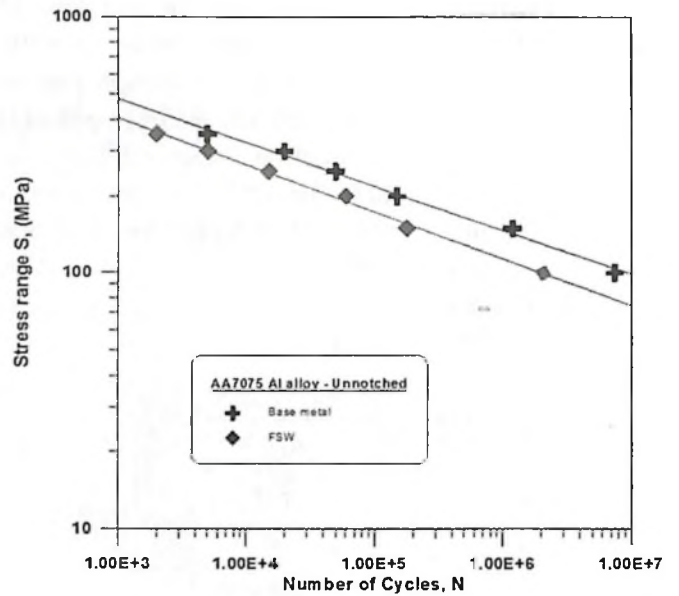


**Fig. 2 : S-N curves of parent metal and FSW joint (unnotched condition)**

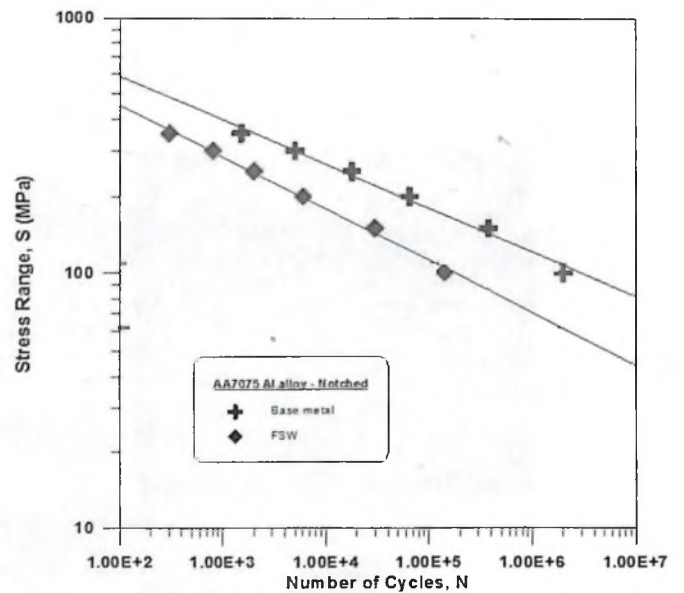


**Fig. 3 : S-N curves of parent metal and FSW joint (notched condition)**

**Table 2 : Fatigue properties of the parent metal and FSW Joint**

	Basquin Constant		Fatigue strength of unnotched specimen, @ 2x10 <sup>6</sup> cycles (MPa)	Fatigue strength of notched specimen, @ 2x10 <sup>6</sup> cycles (MPa)	Fatigue notch factor (k <sub>f</sub> )	Notch Sensitivity Factor (q)
	A	n				
Parent metal	2.96093x10 <sup>12</sup>	2.85	140	115	1.22	0.82
FSW joint	3.91613x10 <sup>13</sup>	3.57	100	62	1.61	0.74

Fig. 3 shows the S-N curves of notched specimen. The data for notched specimens are usually plotted in terms of nominal stress based on the net section of the specimen. The effectiveness of the notch in decreasing the fatigue limit is expressed by the fatigue strength reduction factor or fatigue notch factor,  $K_f$ . The fatigue notch factor for all the joints was evaluated using the following expression [19]

$$K_f = \frac{\text{Fatigue limit of unnotched specimen}}{\text{Fatigue limit of notched specimen}} \quad (2)$$

The notch sensitivity of a material in fatigue is expressed by 'q' and it can be evaluated using the following expression.

$$q = \frac{(K_t - 1)}{(K_f - 1)} \quad (3)$$

Where  $K_t$  is the theoretical stress concentration factor and is the ratio of maximum stress to nominal stress. Using the above

expression, fatigue notch sensitivity factor 'q' was evaluated for all the joints and they are presented in Table 2.

From the results presented in Table 2, it is inferred that the base metal endured more number of cycles than FSW joint. Slope of the S-N curve (Basquin Constant) is another measure to understand the fatigue performance of welded joints. If the slope of the S-N curve is smaller, then the fatigue life will be higher and vice versa. Thus, base metal with a minimum slope (2.8) exhibits maximum endurance stress of 140 MPa than FSW joint. Reduction in fatigue strength due to the presence of circular V-notch was evaluated by fatigue notch factor and the notch sensitivity factor. The notch sensitivity factor of the FSW joints is found to be the higher than the base metal. The notch sensitivity factor of base metal is found to be lower than the FSW joint.

Table 3 : Transverse tensile properties of Parent Metal and FSW Joint

	0.2% Yield strength (MPa)	Ultimate tensile strength (MPa)	Elongation 50 mm gauge length (%)	Notch tensile strength (MPa)	Notch strength Ratio (NSR)	Joint efficiency (%)	Failure location
Base Metal	510	563	16	571	1.01	–	–
FSW Joint	335	394	12	410	1.04	70	ASTMAZ

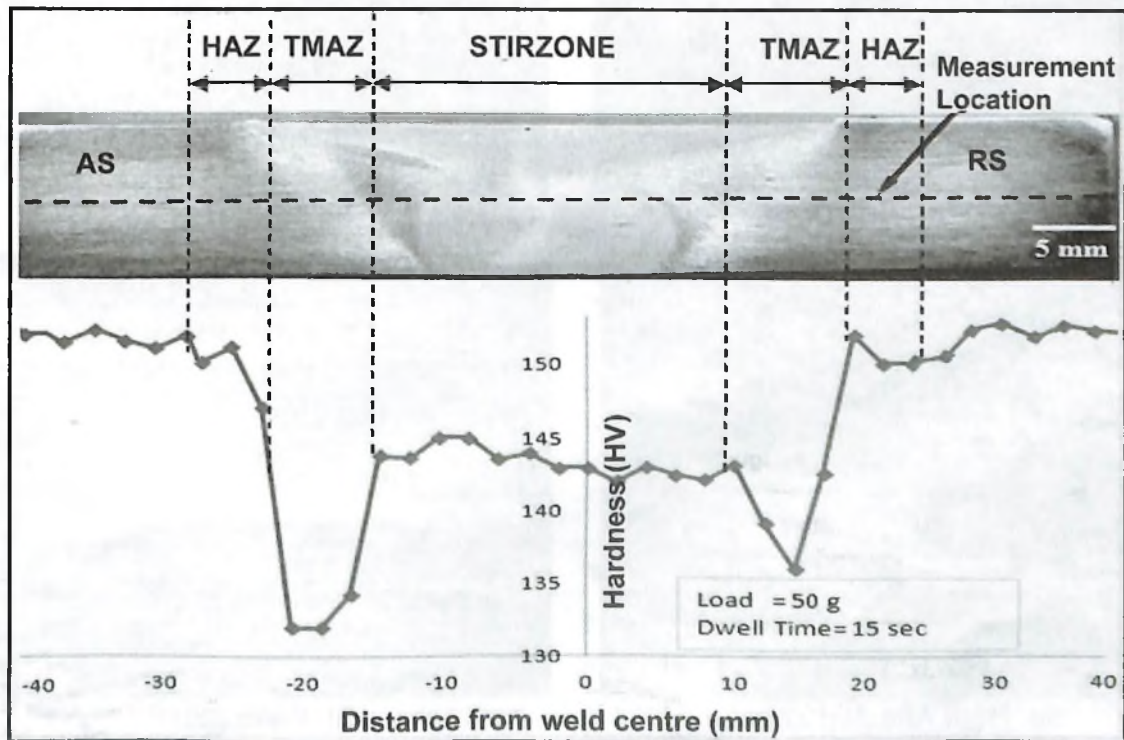
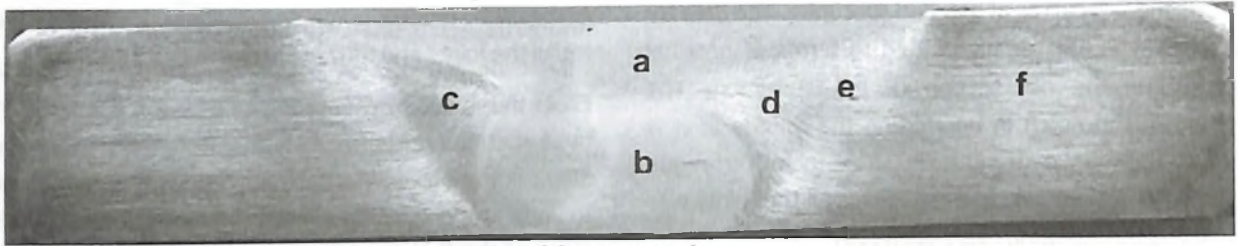
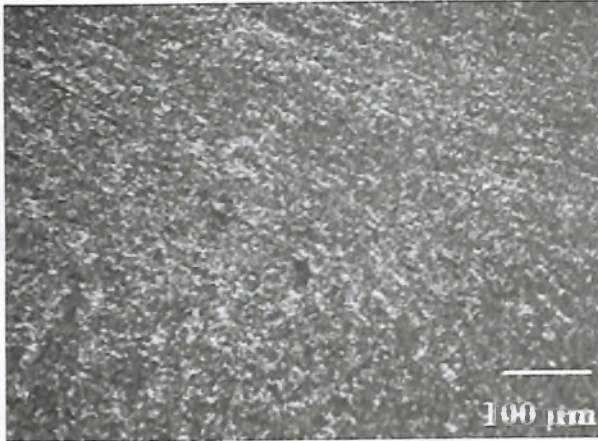


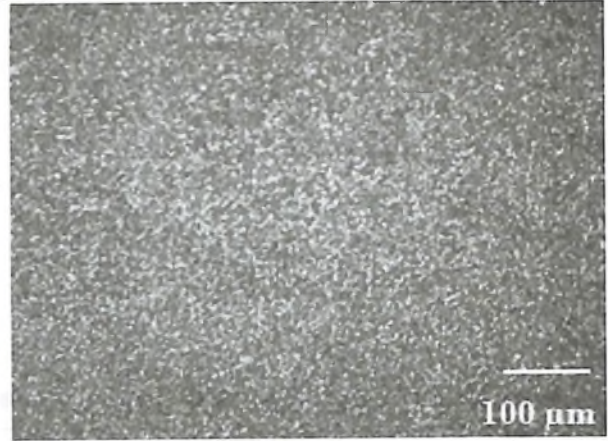
Fig. 4 : Hardness profile across the weld center line (WCL)



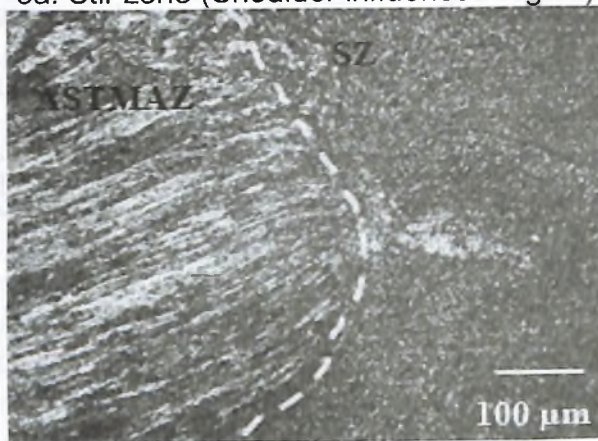
Macrograph



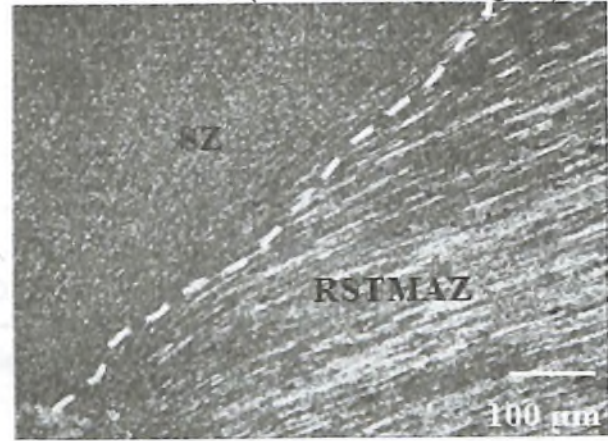
5a. Stir zone (Shoulder influenced region)



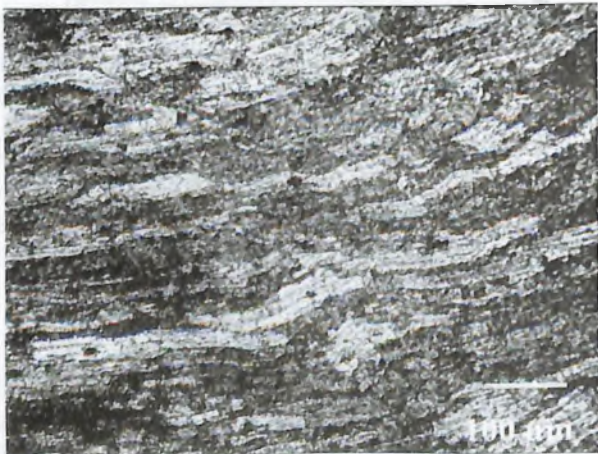
5b. Stir zone (Pin influenced region)



5c. AS - TMAZ



5d. RS - TMAZ



5e. Heat Affected Zone



5f. Base metal

Fig. 5 : Optical micrograph of various regions of FSW Joint

### 3.2 Tensile properties

The transverse tensile properties such as yield strength, tensile strength and percentage of elongation of AA 7075 alloy joints were evaluated. In each condition, three specimens were tested, and the average of three results is presented in **Table 3**. The yield strength and tensile strength of unwelded parent metal are 510, 563 MPa respectively. But the yield strength and tensile strength of as welded joints are 335 and 394 MPa respectively. This indicates that there is a 30 % reduction in tensile strength due to FSW process.

### 3.3 Microhardness

The hardness across the weld cross section was measured along the mid thickness of the joint using a Vickers microhardness testing machine and the results were presented in the graph **Fig. 4**. The hardness profile shows basin like profile indicates that the stir zone undergoes softening due to the heat supplied by the FSW process.

### 3.4 Microstructure

**Fig. 5** illustrates the details of variation of microstructure corresponding to different regime in the macrograph. The microstructure of the welded joint normally divided into the following three regions: the dynamically recrystallized zone (DXZ) or the weld nugget, thermomechanically affected zone (TMAZ), and heat-affected zone (HAZ) [22]. The weld nugget is characterized by a recrystallized, fine equiaxed grain structure because the precipitates have fully or partially gone into solution and re-precipitated during the joining process. The transition zone between the heat-affected zone (HAZ) and the weld nugget is thermo mechanically affected zone (TMAZ) characterized by a highly deformed structure [23].

The weld nugget is composed of fine-equiaxed recrystallized grains, which are formed under the high temperature and high rate of deformation in the weld nugget due to the pins stirring [24], and the size of the crystal grain is very fine. **Fig. 5a** represents the top surface microstructure which shows comparatively coarse grains as compared with **Fig. 5b** bottom zone of the nugget. **Fig. 5c** represents the advancing side thermo mechanically affected zone AS-TMAZ clearly shows that there is an orientation difference in grains in addition with highly deformed microstructure. This could be attributed to the lower hardness observation in this zone as compared to retreating side thermo mechanically affected zone (RS – TMAZ) shown in **Fig. 5d**. Although both the advancing side and the retreating side have a boundary with the weld nugget, the boundary in the advancing side is clearer than that in the retreating side. HAZ microstructure shown in **Fig. 5e** reveals

the presence of coarser microstructure could be attributed to the lower hardness across the zone [23]. **Fig. 5f** represents the microstructure of base metal consisting very fine insoluble second phase precipitates dispersed in various locations of elongated grains. The microstructure was partially recrystallized, with fairly large recrystallized grains that were flattened and elongated in the longitudinal direction as a consequence of the mechanical deformation introduced by the rolling operation.

The recrystallized grain size was non-uniform along each of the three orthogonal directions of the wrought plate, resulting in an anisotropic microstructure. From this microstructural observation it was understood that the weld nugget is characterized by a recrystallized, fine equiaxed grain structure [3-7] because the precipitates have fully or partially gone into solution and re-precipitated during the joining process. There are different grain sizes in depth direction of weld nugget shown in **Fig. 5(a-b)**, respectively. The average grain size at the bottom side of weld is smaller than that of the centre and top sides. This is because that the top side of weld fully contacted with the welding shoulder in the welding progress and thus generated much more heat through the rotating tool shoulder. On the other hand the bottom side directly contacted with the back plate which acted as a heat sink. The difference in grain size could be attributed to the rapid cooling rate resulted in the faster recrystallization procedure on the pin influenced region of weld. So on the shoulder influenced region of weld, there is a crystal grain growth progress during the recrystallization owing to the slow cooling rate.

### 3.5 Fractography

**Fig. 6** represents the fracture surfaces of the unnotched and notched fatigue specimens for the parent metal and FSW joints at the stress level of 100 MPa. **Fig. 6a** represents the scanned image and SEM image of the unnotched parent metal. The scanned image of the parent metal smooth fatigue specimen fracture surface reveals smooth cake cut like fracture surface indicating the slow progress of crack for this low stress. The SEM image of the fracture surface of the parent material smooth fatigue specimen shows intergranular failure with faceted steps.

**Fig. 6b** shows the scanned image and SEM image of the fracture surface of the unnotched FSW joint fatigue specimen. The scanned image of the fracture surface of the unnotched FSW joint shows irregular path of fracture surface which indicates the lower stress levels resulting in multiple crack

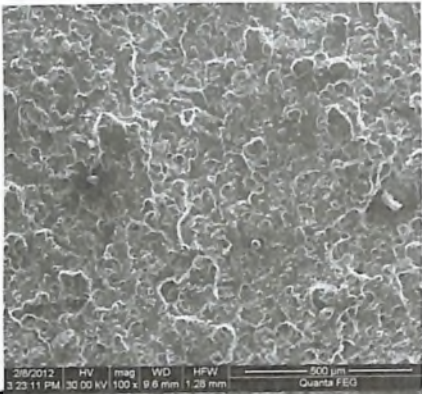
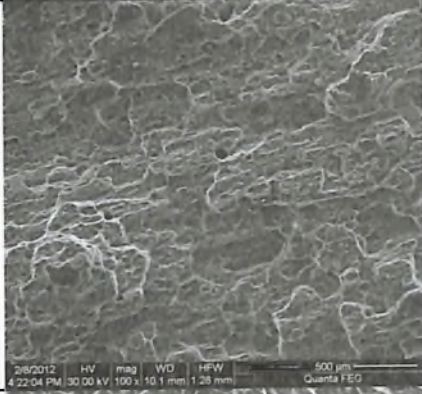
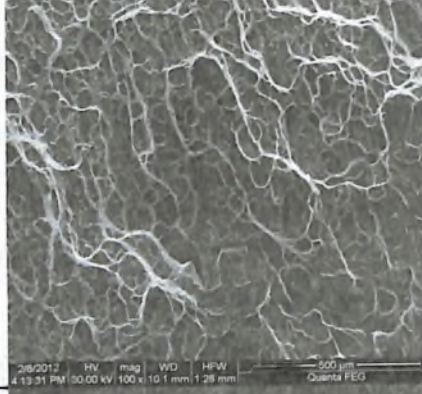
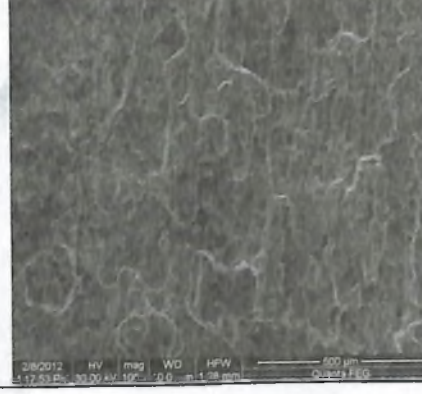
Sl.No.	Condition	Scanned Image	SEM Image	Observation
a	PM Unnotched		 2/8/2012 HV mag WD HFW 3:22:11 PM 30.00 kV 100 x 9.6 mm 1.28 mm 500 µm Quanta FEG	Fracture appearance : Smooth  Failure Type : Intergranular failure
b	FSW Unnotched		 2/8/2012 HV mag WD HFW 4:22:04 PM 30.00 kV 100 x 10.1 mm 1.28 mm 500 µm Quanta FEG	Fracture appearance : Irregular fracture path  Failure Type : Intergranular failure
c	PM Notched		 2/8/2012 HV mag WD HFW 4:13:31 PM 30.00 kV 100 x 10.1 mm 1.28 mm 500 µm Quanta FEG	Fracture appearance : Typical fatigue failure  Failure Type : Fatigue beach marks and tear lips
d	FSW Notched		 2/8/2012 HV mag WD HFW 4:17:53 PM 30.00 kV 100 x 10.1 mm 1.28 mm 500 µm Quanta FEG	Fracture appearance : Bright  Failure Type : Dimples and intergranular facets

Fig. 6 : Fracture surfaces of fatigue specimens

initiation sites. The SEM image of the fracture surface of the unnotched FSW joint which resembles an intergranular failure and the surface is quite complex, with some regions that appear to show clusters of minute dimples and other regions that strongly resemble intergranular fracture.

**Fig. 6c** shows the scanned image and SEM image of the fracture surface of the notched parent metal fatigue specimen. The scanned image of the fracture surface of the notched parent metal fatigue specimen reveals the presence of crack initiation region, propagation region and final failure region, this could be attributed to the higher after cycles of this base metal. The SEM image of the fracture surface of the notched parent metal fatigue specimen reveals the presence of fatigue beach marks in the tear lips.

**Fig. 6d** shows the scanned image and SEM image of the fracture surface of the notched FSW joint fatigue specimen. The scanned image of the fracture surface of the notched FSW joint fatigue specimen shows the bright surface. The SEM image of the fracture surface of the notched FSW joint fatigue specimen reveals the presence of some regions which appear to show dimples while, the other regions that strongly resemble intergranular facets like structure.

#### 4.0 DISCUSSION

The microstructure of parent metal and the joint play a major role in deciding the fatigue properties of this AA7075 -T651 alloy. The microstructures of the weld metal region will have

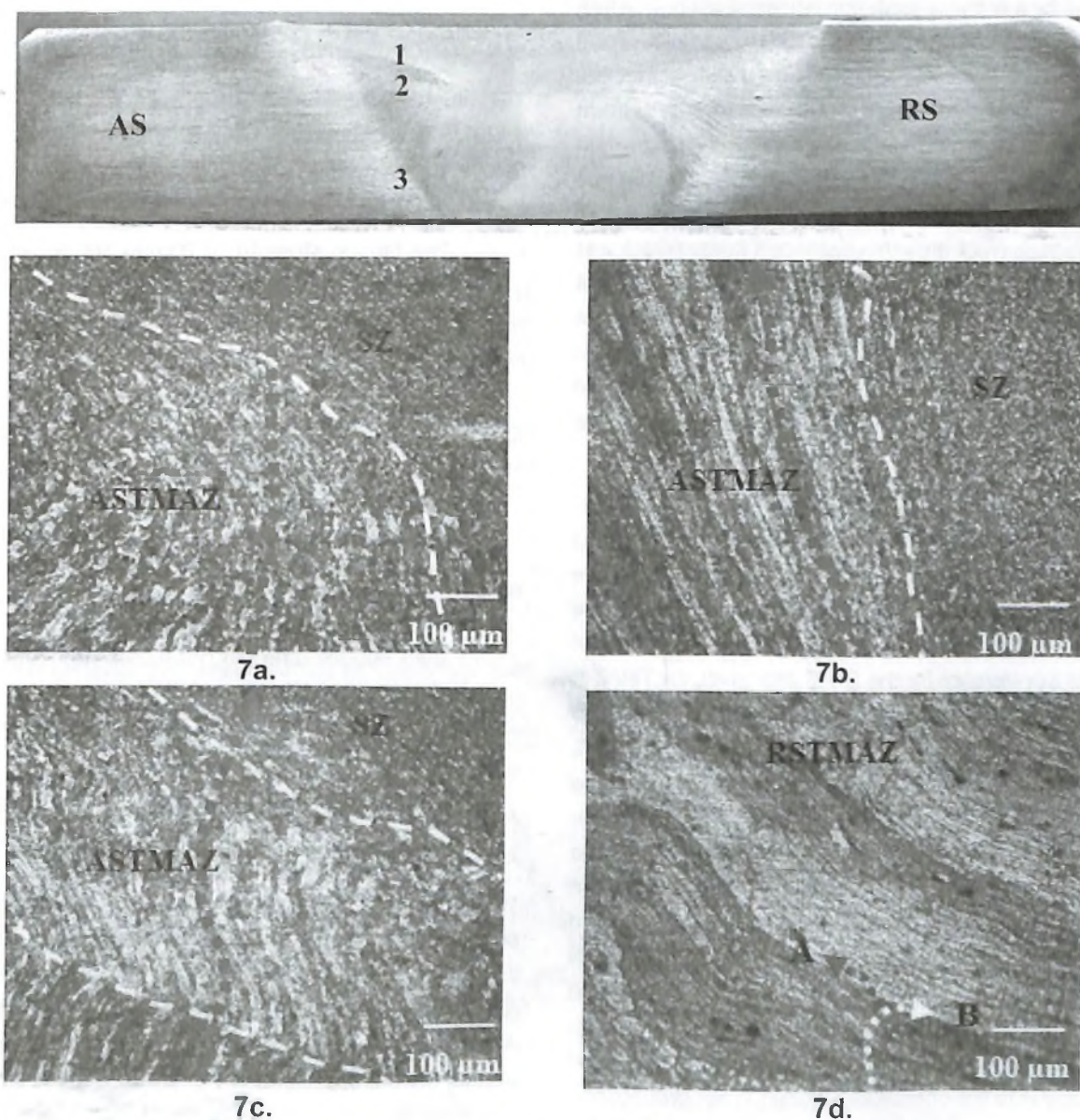


**Fig. 7 : Microstructural Illustration of probable crack path in TMAZ location**

greater influence on the fatigue performance of the joint than weld bead geometry, joint design etc. Microstructure invariably affects the fatigue strength by increasing the propensity for crack nucleation and its early growth, causing the ultimate failure of the joint. In addition to grain size, degree of age hardening, and oxygen content, the fatigue properties of AA 7075-T651 aluminium alloy is strongly influenced by the morphology, size and arrangements of second phase particles in this weld zone determines the fatigue properties of the FSW joint.

Mechanical properties of composite weld structures in this base metal depend on structural characteristics of each weld region, which in turn depend on the specific thermal-mechanical cycles imposed during friction stir welding which is characterized by a recrystallized, fine equiaxed grain structure in addition with fine dispersed second phase particles. From the microstructure it can be seen that the weld nugget are made up of fine and equiaxed grains with fairly uniform distribution features. The grain size is obviously smaller than that of parent material. These features would benefit to fatigue performance with longer initiating life of fatigue micro cracks and higher fatigue crack growth resistance if fatigue crack was produced in the weld nugget. In this way the FSW joints might have equivalent fatigue properties with the base materials, but from the fatigue test results it was observed that the fatigue strength of FSW joints is generally lower than that of base metal and the fatigue fracture is always occurred at the root side of the ASTMAZ of the joints.

In thermo-mechanically affected zone (TMAZ) and heat-affected zone (HAZ), the dynamically recrystallized phenomenon does not occur, but the smaller precipitates have coarsened during welding [25]. The location of initiation is the boundary between the nugget and TMAZ, the location of initiation has a preference for the TMAZ. Moreover, the TMAZ at the advancing side exhibits lower fracture initiation properties than the TMAZ at the retreating side. This asymmetric behaviour is fully attributed to the asymmetric welding process. The microstructure in the weld has direct influence on the appearance of the fracture surface. **Fig. 7** represents the microstructural features at the TMAZ location alone at different location. From **Fig. 7a-7c** the ASTMAZ grains are oriented in the vertical direction due to the combined action of the tool rotation and heat generated by the tool. This is highly assisted for the faster crack initiation and propagation at this zone as illustrated in **Fig. 7a-7c**. In this, the initiated crack can be grown faster due to the orientation of grain, crack propagation

path are parallel and these two are perpendicular to the loading direction. While in RSTMAZ the grain orientation is not so parallel to the crack propagation direction and also the possible crack propagation path could be deviated in both directions as illustrated in **Fig. 7d**. This could be the reason for the failure of specimen was occurred at ASTMAZ. The influence of ASTMAZ microstructure is more predominant than nugget zone, RSTMAZ and HAZ microstructures is the reason for lowering the fatigue properties of this FSW joints as compared with the base metal. Though the fatigue properties of FSW joints are inferior to the base metal fatigue properties due to the above discussed reasons; the fatigue properties of FSW joints can be improved by heat treatments, re-precipitation, and hardening processes in the TMAZ.

## 5.0 CONCLUSIONS

The fatigue behaviour of friction stir welded 12 mm thick AA7075-T651 aluminium alloy joints was investigated and compared with the unwelded parent metal. From this investigation the following important conclusions are derived:

- i. The fatigue strength of friction stir welded AA7075-T651 aluminium alloy joint is 40% lower than unwelded parent metal. This may be due to the lower yield strength (30%) of FSW joint than unwelded parent metal.
- ii. The fatigue failure and tensile fracture occurred in the advancing side of thermomechanically affected zone (AS-TMAZ). This may be due to the presence of softened and coarse elongated grains in AS-TMAZ.
- iii. The influence of ASTMAZ microstructure (grains are oriented in the vertical direction) is more predominant than nugget zone (recrystallized, fine equiaxed grain structure), RSTMAZ and HAZ microstructures is the reason for lowering the fatigue properties of this FSW joints as compared with the parent metal.

## ACKNOWLEDGEMENTS

The authors would like to thank Dr. A. K. Lakshminarayanan for providing support to carry out this investigation. The authors are grateful to the Centre for Materials Joining & Research (CEMAJOR), Department of Manufacturing Engineering, Annamalai University, for extending all the necessary facilities to carry out this investigation.

## REFERENCES

- [1] Balasubramanian, V., Ravisankar, V. and Madhusudhan Reddy, G. (2008); Effect of post weld aging treatment on fatigue behaviour of pulsed current welded AA7075 aluminium alloy joints. *J Mater Eng Perform*, 7(2), pp.224–33.
- [2] Thomas, W. M., Nicholas, E. D., Needham, J. C., Murch, M. G., Temple Smith, P. and Dawes, C. J., The Welding Institute; TWI; PCT World Patent Application WO 93/10935. Filed: 27 Nov. 1992 (UK 9125978.8, 6 Dec. 1991). Publ: 10 June 1993.
- [3] Rhodes, C. G., Mahoney, M. W., Bingel, W. H., Spurling, R. A. and Bampton C. C. (1997); Effects of friction stir welding on microstructure of 7075 aluminium. *Scripta Mater*, 36(1), pp.69-75
- [4] Liu G., Murr, L. E., Niou, C. S., McClure, J. C. and Vega, F.R., (1997); Microstructural Aspects of the Friction Stir Welding of 6061-T6 Aluminum, *Scripta Mater*, 37(3), pp. 355361.
- [5] Murr, L. E., Liu, G. and McClure, J. C., (1998); A TEM Study of Precipitation and Related Microstructures in Friction Stir Welded 6061 Aluminium, *J. of Mater Sci*, 33, pp.12431251.
- [6] Mishra, R. S., Mahoney, M. W., McFadden, S. X., Mara, N. A. and Mukherjee, A. K. (2000); High strain rate superplasticity in a friction stir processed 7075 al alloy, *Scripta Mater*, 42, pp.163-168.
- [7] Li, Y., Murr, L. E. and McClure, J.C. (1999); Solid state flow visualization in the friction-stir welding of 2024 Al to 6061 Al, *Scripta Mater*, 40(9), pp.10410-1046
- [8] Dickerson, T. L. and Przydatek, J. (2003); Fatigue of Friction Stir Welds in Aluminium Alloys that Contain Root Flaws, *Int. J. of Fatigue*, 25, pp.1399-1409.
- [9] Lomolino, S., Tovo, R. and Dos Santos, J. (2005); On the fatigue behavior and design curves of friction stir butt-welded Al alloy, *Int. J. Fatigue*, 27, pp.305-316.
- [10] James, M. N., Hattingh, D. G. and Bradley, G. R. (2003); Weld tool travel speed effects on fatigue life of friction stir welds in 5083 aluminium, *Int. J. of Fatigue*, 25 pp.1389-1398
- [11] Malarvizhi, S. and Balasubramanian, V. (2011); Effect of welding processes on AA2219 aluminium alloy joint properties *Trans. Nonferrous Met. Soc. China*, 21, pp.962-973.
- [12] Cavaliere, P., Nobilea, R., Panellaa, F. F. and Squillace, A. (2006); Mechanical and Microstructural Behaviour of 2024-7075 Aluminium Alloy Sheets Joined by Friction Stir Welding, *Int. J. of Machine Tools Manufac*, 46, pp.588–594.
- [13] Tianwen Zhao and Yanyao Jiang (2008); A study of fatigue crack growth of 7075-T651 aluminum alloy *Int. J. Fatigue*, 30, pp.834-849.
- [14] Caizhi Zhou, Xinqi Yang and Guohong Luan, (2005); Fatigue properties of friction stir welds in Al 5083 alloy, *Scripta Materialia*, 53, pp.1187-1191.
- [15] Cavaliere, P., De Santis, A., Panella, F. and Squillace A. (2009); Effect of anisotropy on fatigue properties of 2198 Al-Li plates joined by friction stir welding, *Engg Failure Analysis*, 16, pp.1856–1865.
- [16] Srivatsan, T. S., Anand, S., Sriram, S. and Vasudevan, V. K. (2000); "The high-cycle fatigue and fracture behavior of aluminium alloy 7055, *Mater Sci and Engg: Series A*, A281, pp.292-304.
- [17] Temmar, M., Hadji, M. and Sahraoui, T. (2011); Effect of post-weld aging treatment on mechanical properties of Tungsten Inert Gas welded low thickness 7075 aluminium alloy joints, *Mater and Design*, 32, pp.3532–3536.
- [18] Lakshminarayanan A. K. and Balasubramnaian, V. (2008); The mechanical properties of the GMAW, GTAW and FSW joints of the RDE-40 aluminium alloy, *Int. J. of Microstructure and Mater. Properties*, 3(6), pp.837-853.
- [19] Sonsino, C. M. (1999); Fatigue assessment of welded joints in Al-Mg-4.5 Mn aluminium alloy AA 5083 by local approaches, *Int. J. Fatigue*, 21, pp.985-999
- [20] George Dieter, E. (1988); *Mechanical Metallurgy*. 3rd edition, McGraw-Hill, Publishing, New York, pp.376–431.
- [21] Liu, H. J., Fujii, H., Maeda, M. and Nogi, K. (2003); Heterogeneity of mechanical properties of friction stir welded joints of 1050-H24 aluminium Alloy, *J. Mater. Sci. Lett.*, 22, pp.441-444.
- [22] Singh, R. K. R., Chaitanya Sharma, D. K., Dwivedi, N. K. and Mehta, P. Kumar, (2011); The microstructure and mechanical properties of friction stir welded Al-Zn-Mg alloy in as welded and heat treated conditions, *Mater. and Design* 32, pp.682–687.
- [23] Jata, K. V. and Semiatin, S. L. (2000); Continuous dynamic recrystallization during friction stir welding of high strength aluminium alloys, *Scripta Materialia*, 43(8), pp.743749.
- [24] Caizhi Zhou, Xinqi Yang and Guohong Luan, (2005); Fatigue properties of friction stir welds in Al 5063 alloy, *Scripta Materialia*, 53, pp.1167–1191.
- [25] Jata, K. V., Sankaran, K. K. and Ruschau, J. (2000); Friction stir welding effects on microstructure and fatigue of aluminium alloy 7050- T7451, *Metallurgical and Mater. Trans.*, 31A, pp.2181-2192.